Highlights

Understanding the Behaviour of Motorcycle Riders: An Objective Investigation of Riding Style and Capability

Mirco Bartolozzi, Abderrahmane Boubezoul, Samir Bouaziz, Giovanni Savino, Stéphane Espié

- Objective assessment of motorcyclists' familiarisation, riding style, and capability
- Correlation found between rider experience and motorcycle dynamics intensity levels
- Riders converge to their capability level through familiarisation
- Clustering approach identified trial groups based on motorcycle dynamics and rider inputs
- Riding instructions influence rider behaviour, particularly in terms of input usage

Understanding the Behaviour of Motorcycle Riders: An Objective Investigation of Riding Style and Capability

Mirco Bartolozzi[a,*], Abderrahmane Boubezoul[b], Samir Bouaziz[c], Giovanni Savino[a], Stéphane Espié[b]

[a] *Department of Industrial Engineering, University of Florence, Via di Santa Marta 3, Florence, 50139, Tuscany, Italy*
[b] *TS2/SATIE/MOSS, Université Gustave Eiffel, Champs-sur-Marne, 77420, France*
[c] *SATIE/MOSS, Université Gustave Eiffel, ENS Paris- Saclay, CNRS, Gif-sur-Yvette, 91190, France*

Abstract

Human errors are the primary cause of powered two-wheeler crashes worldwide due to the demanding control required and the often ineffective rider-training programs. Literature on rider behaviour is limited, partly due to the lack of standard investigation methodologies.

This work investigated the differences in riding style and capability of a diverse set of riders. It explored the impact of familiarisation and riding instruction through objective metrics. Correlation with experience was a particular focus.

Seven riders of various experience levels performed trials on an instrumented motorcycle, following three riding instructions: 'Free Riding', 'Handlebar Riding', and 'Body Riding'. Objective metrics assessed rider familiarisation, capability and willingness to excite motorcycle dynamics, riding style, and input preference.

Results indicated that riders asymptotically converged to their motorcycle dynamics intensity level after a specific distance; both intensity and distance were positively correlated with experience. Experienced riders achieved higher

*Corresponding author
Email addresses: mirco.bartolozzi@unifi.it (Mirco Bartolozzi), abderrahmane.boubezoul@univ-eiffel.fr (Abderrahmane Boubezoul), samir.bouaziz@universite-paris-saclay.fr (Samir Bouaziz), giovanni.savino@unifi.it (Giovanni Savino), stephane.espie@univ-eiffel.fr (Stéphane Espié)

longitudinal acceleration and utilised combined dynamics to a higher degree. The negative longitudinal jerk during braking varied greatly among riders and correlated with experience. A clustering approach identified two prominent trial groups concerning the motorcycle response intensity. Higher diversity emerged in the inputs, leading to five clusters with distinct riding style meanings. Instructions influenced behaviour, particularly regarding input usage.

The unsupervised approach and metrics proposed should make rider behaviour research more straightforward and objective. It could be applied to naturalistic riding sessions for more conclusive evidence of inter-driver differences. The diversity that emerged concerning the command inputs used warrants a revision of training practices to promote riding safety.

Keywords: Powered two-wheeler rider behaviour, Riding profiles, Motorcycle dynamics, G-g diagram, Data mining, Research methods

1. Introduction

Powered Two-Wheelers (PTWs), encompassing motorcycles, mopeds, and scooters, have become increasingly numerous worldwide (Terranova et al., 2022). While assistance systems and technological advancements have improved road safety, PTWs still carry a higher risk than other modes of transportation, with riders being more susceptible to severe injuries and fatalities in accidents (Beck et al., 2007; Brown et al., 2021).

Global in-depth studies consistently attribute the primary cause of PTW crashes to the human factor (ACEM, 2008; Hurt et al., 1981). Various studies have found some rider training programs ineffective, emphasising the need for improved training design (Ivers et al., 2016; Savolainen and Mannering, 2007). To further reduce injury and fatality rates, it is crucial to comprehend the human-vehicle interaction. This understanding, which is useful for the development of any active assistance system, becomes even more crucial for the development of systems acting on the steering, which could, in the future, reduce injuries in a significant portion of accidents involving such vehicles (Bartolozzi et al., 2023b). A data-driven approach based on monitoring, recording, and analysing rider behaviour facilitates its understanding (Vlahogianni et al., 2011).

Literature on riding behaviour is limited (Diop et al., 2020). Most studies focus on the inter-rider difference regarding vehicle dynamics, independent of the input causing it. Hisaoka et al. studied the driver-vehicle system behaviour through the g-g diagram, a scatter plot combining lateral and longitudinal acceleration (Hisaoka et al., 1999). In particular, they generalised the friction ellipse through the 'capability envelope' concept by recognising that the human constitutes an additional limiting factor. Not only is the maximum measured acceleration achieved lower than the physical limit, but the curve is not necessarily an ellipse. A subjective trial-and-error process determined the exponent characterising the capability envelope shape. The concept, first defined concerning cars, can also be applied to PTWs. Biral et al. followed a similar approach to determine the exponent; then, they determined the maximum longitudinal and lateral acceleration values as those that let the envelope contain 99% of the data points: however, multiple combinations of these two parameters satisfy the threshold (Biral et al., 2005). Will et al. analysed professional and non-professional riders' behaviour in a naturalistic environment using the g-g diagram (Will et al., 2020). They highlighted the qualitative difference between the diagram's three typical shapes and their correlation with experience[1]. Some statistical features of the trials belonging to each group were computed and discussed, yet, the clustering process was manual and subjective. Even though these studies highlighted the g-g diagram's usefulness in investigating each rider's capability[2], they did not propose a method to objectively and automatically determine the capability envelope.

[1]In the present article, 'experience' refers to the comprehensive assessment of an individual's knowledge, skills, proficiency, and practical understanding acquired through an extended period of active motorcycle riding, training, and exposure to various riding conditions.

[2]'Capability' refers to the rider's tendency to demand and sustain high degrees of vehicle dynamics, i.e. in terms of acceleration and its rate of change.

Some studies compared the behaviour of different riders using additional signals. Magiera et al. assessed riding skill through the standard deviation of high-pass filtered roll rate signal (Magiera et al., 2016). The process was unsupervised; however, the two cut-off frequencies[3] were chosen heuristically, and no indication was provided on generalising their selection. Diop et al. clustered the trials of different riders using the statistics of the roll angle and its derivatives; the unsupervised approach proposed is promising and should be applied to a broader range of signals (Diop et al., 2023).

Studies investigating the influence of a specific riding instruction are rare. In another article, Diop et al. studied the behaviour of eight riders subject to different riding instructions (Diop et al., 2020). The study highlighted that differentiating between instructions is challenging and that various riding practices are possible. Limitations of the study are that the riders were all gendarmes and that the clustering considered only the signals describing the motorcycle response and not the specific inputs applied by the rider, which should be more indicative of the riding preference. No study automatically categorised riders under different instructions based on the rider inputs.

A better understanding of motorcyclists' behaviour, identifying the most common lack of skills and highlighting the main areas of improvement for a given subject would improve traffic safety by supporting preventive actions, like enhancing or re-designing training programs (Huertas-Leyva et al., 2021). To overcome these gaps, this article investigates the differences in riding style[4] and capability of a diverse set of riders, considering any potential riding instructions provided and the effect of the familiarisation[5] process. These differences are to

[3]One frequency for stationary riding and another for dynamical manoeuvres.

[4]'Riding Style' is defined as the unique way a rider performs a manoeuvre type, i.e. entering a corner. It encompasses body positioning and movement, acting on the steering, how the throttle and brake are used, and their general approach to riding. It is an aspect of the broader concept of 'rider behaviour'.

[5]'Familiarisation' is defined as the process of becoming acquainted with a vehicle, its controls, and the surrounding driving environment to operate it safely and effectively.

be sought not only in the PTW response but also in the actions that cause it, many of which (such as the forces applied to the footpegs) have little impact on the dynamics but can be used for psychological and comfort reasons (Weir, 1972). Therefore, the study also has a methodological purpose, whereby methods must be automated and objective to be easily reproduced. All evidence must be compared with the experience level and possible correlations discussed.

The paper structure follows: Section 2 describes the experimental protocol and the participants, the instrumented motorcycle and reference frame, the metrics used to describe the familiarisation process and rider capability, and the clustering process. Section 3 presents the investigation results, which are further discussed in Section 4 also concerning their broader meaning. Lastly, Section 5 summarises the conclusions and implications and discusses the potential applications and areas of interest for this study.

2. Materials and Methods

2.1. Experimental Test Description

The riding data was obtained through an instrumented sports touring motorcycle (Honda CBF 1000) during an experimental test campaign on a section of the La Ferté-Gaucher track; a single trial of that dataset was used in another study having a completely different purpose (Bartolozzi et al., 2023a). Seven riders were involved, having vastly different experience levels. The declared licence age and distance travelled in the previous year, used as a proxy for their experience level, are given in Table 1. Each rider was also asked to state their preference concerning riding using mainly the handlebar or mainly the body; the answers are found in the table. One rider (S_2) was still in the process of getting his riding licence at the time of the experiment. Another one (S_7) was a professional trainer of riding trainers. Six riders were male, and one (S_1) was female.

Each subject performed three runs for each of three different riding instructions: Free-Riding (FR), Body-Riding (BR) and Handlebar-Riding (HR), for a total of $7 \times 3 \times 3 = 63$ trials. The free-riding instruction preceded the other two, whose order differed among riders (shown in the rightmost column of Table 1). It allowed the rider to familiarise themself with the vehicle and the track and investigate their natural riding approach, as no specific instruction was provided. Concerning the BR trials, the rider was instructed to ride using their body movements (foot, buttocks, knees) primarily; the rider was, instead, instructed to use the handlebar to negotiate bends during the HR runs. Each trial was referred to using the following naming convention: $S_i\{FR/BR/HR\}_j$, indicating the j-th repetition of the FR/BR/HR trial for the i-th rider. The test aimed to compare the riding style of riders with different experience levels and stated preferences, and the impact of the instruction given. Figure 1a illustrates the trajectory of one generic trial. No additional instruction was given concerning the second or third repetition of each instruction type, so they were nominally identical to the first one.

Table 1: Subjects' declarative data acquired before the test, including the Licence Age LA and the distance travelled on a motorcycle during the previous year d. $\text{Handl}_{\text{tot}}$ is the average of the scores given by the rider to riding 'using the handlebar' and 'counter-steering'. Body_{tot} is the average of the scores given by the rider to riding 'moving the body', 'applying pressure on the tank', and 'pushing the footpegs'. The ratio between the two is also shown. A $0-10$ scale was used, with higher numbers indicating higher preference. The order of the instruction received is shown in the rightmost column.

	Experience		**Preference Score**			
Subj	LA (years)	d (km)	$\text{Handl}_{\text{tot}}$ (-)	Body_{tot} (-)	Ratio (-)	Order
S_1	10	0	8.0	5.9	1.36	FR,HR,BR
S_2	0	0	8.0	5.8	1.38	FR,HR,BR
S_3	9	25000	8.8	7.0	1.26	FR,HR,BR
S_4	5	2000	8.2	8.3	0.99	FR,BR,HR
S_5	2	8000	5.2	8.4	0.62	FR,HR,BR
S_6	1	6000	6.5	6.7	0.97	FR,BR,HR
S_7	19	5000	9.3	3.3	2.82	FR,BR,HR

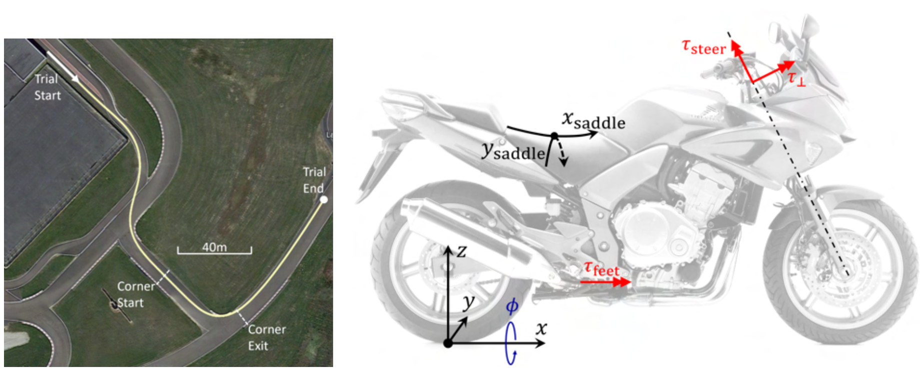

(a) The trajectory of one trial. (b) The coordinate system and the quantities used.

Figure 1: Information on the experiment conducted.

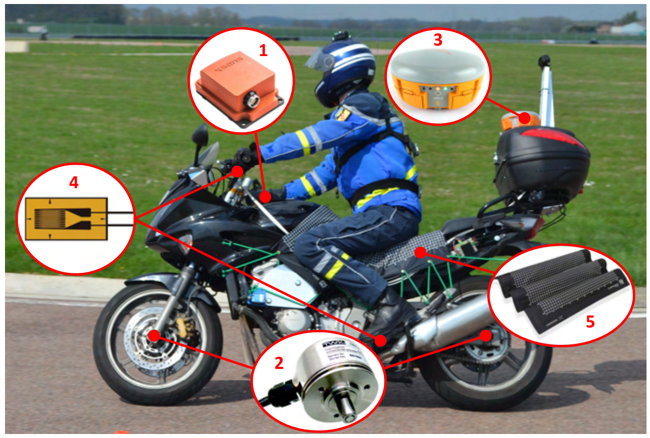

Figure 2: The instrumented motorcycle. The annotations show each sensor's placement.

2.2. Signals and Reference Frame

The instrumented motorcycle and the sensors used are shown in Figure 2; each sensor type is denoted by a number. Several sensors acquired the dynamic state of the motorcycle. Concerning the signals used in the analysis:

- The longitudinal acceleration a_x and lateral acceleration a_y were provided by an MTi Xsens IMU[6] (1), which also measured the motorcycle roll angle ϕ.
- The Hall-effect sensor (2) on the rear wheel provided the travelling speed reading v.
- A GNSS-RTK (Septentrio Altus APS3G[7]) (3) acquired the vehicle coordinates. These were used to compute the travelled distance s.

Additional sensors acquired information about the rider-motorcycle interaction. In particular:

[6] https://www.xsens.com/products/mti-100-series.

[7] https://www.septentrio.com/en/products/gnss-receivers/rover-base-receivers/smart-antennas/aps3g.

- Four Strain gauges (4) are placed on the right and left half-handlebars to measure the longitudinal and vertical forces acting on them. The resulting torque produced by these forces was computed. As the inclination of the steering axis (the caster angle) was known, this torque was projected along the steering axis, obtaining the steering torque τ_{steer}, and perpendicularly to it, obtaining the 'perpendicular torque' $\tau_{\perp}$. τ_{steer} is the primary input for lateral motorcycle dynamics as it is responsible for the steering (Bartolozzi et al., 2023c; Weir and Zellner, 1978); instead, $\tau_{\perp}$ produces no steering action, but it will induce a relative angle between the two, as it is a torque at the interface between the rider and the motorcycle.

- Strain gauges (4) acquired the force the rider exerted on each foot-peg; this was used to compute the rolling torque the rider produced through their feet τ_{feet}.

- A large pressure matrix pad (XSENSOR[8] PX100) (5) acquired the pressure distribution over the saddle in the curvilinear coordinates mapped over it. This information was used to compute the coordinates $\mathrm{CoP}_{x,y}$ of the Centre of Pressure.

The sensors were non-invasive and did not appear in the rider's field of view. The only clearly visible sensors were the pressure pad and the GNSS receiver. The subjects were told that data relative to rider behaviour would be acquired, without further details not to influence their behaviour. The signals were recorded through a data logger and were down-sampled to the joint 10 Hz sampling frequency; each signal was timestamped during recording so that synchronisation would not introduce errors. In the analysis, the dataset corresponding to each trial began when the motorcycle speed exceeded $3\,\mathrm{m\,s^{-1}}$ at the start and stopped when the speed became lower than $3\,\mathrm{m\,s^{-1}}$ at the end, to remove time instants relative to the motorcycle travelling very slowly that would introduce non-representative data.

[8] https://www.xsensor.com/body-pressure-sensors.

This work is data-driven and uses peculiar sensing equipment; data accuracy was crucial, so they have been thoroughly validated by leveraging conceptual and physical models linking the measurements of the various sensors. A few notable examples are provided in this paragraph. Lateral acceleration, the product between the yaw rate and the travelling speed, and the tangent of the roll angle multiplied per the gravity of the Earth were very close in value, as expected: $a_y \approx \dot{\psi}v \approx -\tan\phi/g$. The lowest correlation between the three was $R = 0.945$, which is extremely high considering that the relationship is approximately true only in steady-state conditions. The measured longitudinal acceleration was very close to the time derivative of the travelling speed signal. In straight riding, the difference between the speed measured by the GNSS and that sensed by each wheel's Hall effect sensor was negligible. The variability in steering torque was explained mainly by the roll angle and roll rate, as simplified models predicted (Bartolozzi et al., 2023b). The total vertical force sensed by the rider-motorcycle interfaces (handlebar, saddle and footpegs) approximately equalled each rider's weight on the straights and increased when cornering due to the additional pressure generated by the apparent centrifugal force; the increase followed that predicted by the theory (Figure 3b). The sum of the longitudinal forces applied on the two handlebars was strongly correlated with the longitudinal acceleration (Figure 3a, in blue). This relationship held concerning the vertical forces (shown in orange), too; therefore, the longitudinal and lateral forces were also correlated, and the ratio between the variation of each depended on the rider's height, which dictated the position of their arms. On the straights, the steering torque, perpendicular torque, and torque at the footpegs were about zero on average. For all runs, the average lateral position of the centre of pressure was on the saddle's centerline. The average longitudinal position depended on the rider's stature and did not change based on the instruction given.

Figure 1b shows the signs convention used. A non-tilting reference frame was used to express the acceleration: the forward x and leftward y axes belonged to the ground plane, independent of the motorcycle pitch and roll angles. There-

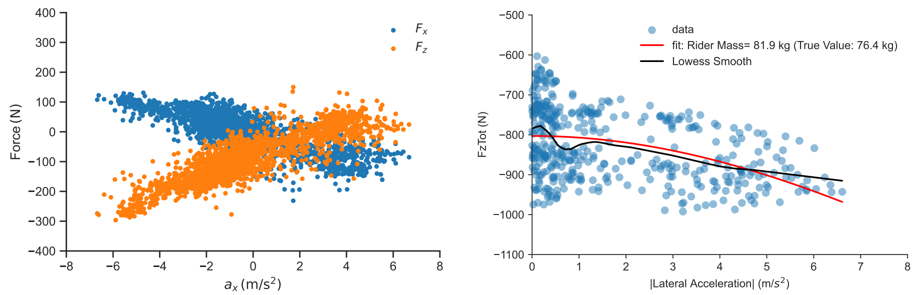

(a) Resulting longitudinal and vertical forces acting on the handlebar for different longitudinal acceleration values (Subject 3).

(b) Total vertical force sensed by the rider-motorcycle interfaces for different intensities of the lateral acceleration. The fit using the theoretical relationship (in red) provides a mass value close to the actual value for that rider (Subject 7).

Figure 3: Examples of the general approach used to verify the correctness of the data acquired.

fore, a_x and a_y acceleration components described the change of the magnitude and direction of the velocity, respectively. As x pointed forwards, the roll angle ϕ was positive when the motorcycle was tilted to the right; similarly, τ_{feet} was positive when it tended to make the motorcycle roll to the right. A positive CoP_x value meant the rider's buttocks were placed forward compared to the saddle centre; a positive CoP_y value indicated a leftward movement over the saddle. The steering torque τ_{steer} was defined around the steering axis and was positive when pointing upwards. The perpendicular torque $\tau_{\perp}$ was positive when it tended to roll the motorcycle to the right. For most riding conditions, the steering torque that the rider applies has the same sign as the roll rate. When the roll angle is positive (rightward corner), or the rider is leaning towards the right, the steering torque is positive (anti-clockwise): this phenomenon is called 'counter-steering'.

2.3. Proposed Metrics

2.3.1. Familiarisation

First, a quantitative description of the familiarisation process was of interest. The first three trials for each rider were relative to the FR instruction, so they were ideal for assessing it. In general, different riders will be confident in reaching different longitudinal and lateral acceleration values; moreover, the same rider will build confidence along the ride and should become confident in reaching higher acceleration values.

The area of the g-g diagram is proposed in this article as a synthetic indicator of rider dynamics performance: a larger area indicates that the rider reached higher acceleration values. Concerning familiarisation, this work proposed tracking the g-g diagram area growth as a function of the distance travelled since the beginning of the first FR trial.

The process to compute it follows. The corresponding k-th couple (a_y^k, a_x^k) is added as a point on the diagram for each new time instant. The convex envelope is computed as the smallest convex polygon that contains the set of n acceleration couples produced up to that point. The polygon will have $Q \leq n$ vertices, each one having coordinates $P_q = (x_q, y_q), q = 1, \ldots, Q$. Notice that $P_{Q+1} = P_1$. Its area A is then determined through the so-called 'triangle formula' formula that transverses its vertices in order (e.g. clockwise) (Abreu de Souza et al., 2018):

$$A^n = \frac{1}{2} \sum_{q=1}^{Q(n)} \left(x_q y_{q+1} - x_{q+1} y_q\right). \tag{1}$$

As the trial progresses, more points are added to the diagram, so by definition, the area computed through Equation (1) is non-decreasing. This area, which measures the extension of the 'rider-capability envelope', is bounded between zero and the friction envelope of the vehicle, which contains the set of physically feasible accelerations; therefore, one expects this area to asymptotically converge to a value A^* lower than the theoretical limit given by the friction envelope. In particular, the increase should be quicker at the beginning, when the area of the envelope is smaller, compared to towards the end of the trial, where increasing the area further requires going beyond now-higher acceleration values. This fact suggests that the g-g diagram area as a function of distance s evolves following a negative exponential function:

$$A(s) = A^* \left(1 - e^{-s/s^*}\right), \tag{2}$$

where s^* is a constant indicating the distance travelled to reach $1-e^{-1} \approx 63.2\%$ of the asymptotic value A^*.

2.3.2. Rider-Capability Envelope

After an initial familiarisation, each rider will reach longitudinal and lateral acceleration values based on their confidence and experience. While the area A of the rider-capability envelope is a synthetic indicator, riders could differentiate also based on the shape of the diagram: a given area could be produced by different combinations of maximum lateral and longitudinal acceleration; moreover, one rider could have a smaller performance envelope despite reaching higher maximum acceleration values by using the combined dynamics to a lower degree.

In general, the rider-capability envelope can be approximated by the following inequality (Hisaoka et al., 1999):

$$\left(\frac{|a_x|}{a_{x\max}}\right)^m + \left(\frac{|a_y|}{a_{y\max}}\right)^m \leq 1, \tag{3}$$

where $a_{x,y\max} = \max_k |a_{x,y}|$ (k is the generic data time index of the concatenated trials considered) are called 'capable longitudinal/lateral acceleration' and determine the length of the two envelope axes and $m > 0$ is the 'capability exponent', which commonly assumes values between 1 (the envelope is a rhombus; the rider monitors the <u>sum</u> of the two acceleration components) and 2 (the envelope is an ellipse); the rider monitors the <u>magnitude</u> of the resulting acceleration vector, as in the case of the friction ellipse). Higher $a_{x,y\max}$ values indicate confidence in reaching higher uncombined acceleration values; a higher m value means the rider used the combined dynamics more frequently and to a higher degree.

The proposed process to derive the rider-capability envelope follows. For each rider, $a_{x,y\max}$ are computed; then, m is determined as the smallest value that makes the rider-capability envelope enclose a fraction of the time instants higher than a threshold (set to 0.98, a trade-off between encompassing the higher acceleration values and making the shape obtained robust concerning possible outliers[9]). The inequality describing the capability envelope is now determined, and four metrics can be derived from it: its area A, the capable longitudinal and lateral acceleration $a_{x,y\max}$, and the capability exponent m. The area is equal to:

$$A = 2\int_{-a_{x\max}}^{+a_{x\max}} a_x(a_y)\, da_y,\;\; a_x(a_y) = a_{x\max}\sqrt[m]{1-\left(\frac{|a_y|}{a_{y\max}}\right)^m}. \qquad (4)$$

The process was then repeated using the jerk[10] values, proposing what in this article is referred to as the J-J diagram. While the g-g diagram informs about the steady-state limits of the dynamics, the J-J diagram describes how quickly the state moves inside the g-g diagram. In the case of the jerk, it was found that the maximum negative longitudinal values were higher than the maximum positive longitudinal values. For this reason, when expressed in terms of the jerk, Equation (1) was split between an upper and lower bound.

It was expected to find some correlation between rider experience and capability; a metric expressing each was defined to assess that. The 'Experience Factor' was defined for the i-th rider by taking into account both their motorcycle Licence Age LA and the distance travelled on a motorcycle in the last year d:

$$\mathrm{expFactor}_i = \frac{1}{2}\left(\frac{\mathrm{LA}_i}{\mathrm{LA}_{\max}} + \frac{d_i}{d_{\max}}\right) \in [0,1],\;\; \mathrm{LA}_{\max} = \max_i \mathrm{LA}_i,\;\; d_{\max} = \max_i d_i. \qquad (5)$$

A factor indicating the rider's willingness to use intense dynamics was also

[9]The threshold was set through trial and error. This threshold is lower than that used by Biral (0.99), as that study used data relative to real roads, where values relative to low acceleration values are over-represented compared to the current article (Biral et al., 2005).

[10]The jerk is the time derivative of the acceleration.

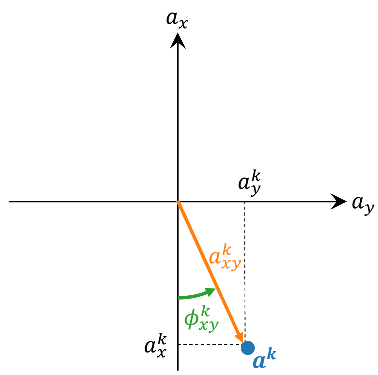

Figure 4: Scheme showing the meaning of the angle ϕ_{xy}^k, which is the angle between the generic k-acceleration vector $\boldsymbol{a}^k = (a_y^k, a_x^k)$ and the closest semi-axis, which is the negative portion of the vertical axis in the case shown.

defined using the following metrics. $\overline{a_{xy}}_i$ is the average total acceleration, each point's distance from the centre of the g-g diagram. $\overline{\phi_{xy}}_i$ is the average angular distance of each point from the closest semi-axis in the g-g diagram, weighted using the total acceleration as weight: a value of 0 would indicate that the rider never produced longitudinal and lateral acceleration at the same time, while a $\pi/4$ value would indicate that the longitudinal and lateral acceleration always had the same value. Lastly, $\overline{J_{xy}}_i$ is analogous to $\overline{a_{xy}}_i$, but in terms of jerk. Refer to Figure 4 for a graphical representation of the a_{xy}^k, ϕ_{xy}^k values for the generic k-th data-point. The three metrics are computed using the following formulae:

$$\overline{a_{xy}}_i = \underset{k}{\text{mean}}\ a_{xy_i}^k \geq 0,\ a_{xy} = \sqrt{(a_x)^2 + (a_y)^2}, \tag{6}$$

$$\overline{\phi_{xy}}_i = \frac{\sum_k \phi_{xy_i}^k a_{xy_i}^k}{\sum_k a_{xy_i}^k} \in \left[0,\ \frac{\pi}{4}\right],\ \phi_{xy} = \begin{cases} \arctan\left|\frac{a_x}{a_y}\right|, & \text{if } |a_x| < |a_y| \\ \arctan\left|\frac{a_y}{a_x}\right|, & \text{if } |a_x| > |a_y| \\ 0, & \text{otherwise} \end{cases} \tag{7}$$

$$\overline{J_{xy}}_i = \underset{k}{\text{mean}}\ J_{xy_i}^k \geq 0,\ J_{xy} = \sqrt{(J_x)^2 + (J_y)^2}. \tag{8}$$

The three indicators were then combined into a single metric, called 'Confidence Factor' expressing the willingness the rider had to excite the motorcycle dynamics to a higher degree:

$$\begin{aligned}\text{confFactor}_i = \frac{1}{3}\Bigg(& \frac{\overline{a_{xy}}_i - \overline{a_{xy}}_{\text{min}}}{\overline{a_{xy}}_{\text{max}} - \overline{a_{xy}}_{\text{min}}} \\ & + \frac{\overline{\phi_{xy}}_i - \overline{\phi_{xy}}_{\text{min}}}{\overline{\phi_{xy}}_{\text{max}} - \overline{\phi_{xy}}_{\text{min}}} + \frac{\overline{J_{xy}}_i - \overline{J_{xy}}_{\text{min}}}{\overline{J_{xy}}_{\text{max}} - \overline{J_{xy}}_{\text{min}}}\Bigg) \in [0,\, 1]\,,\end{aligned} \tag{9}$$

where 'max' and 'min' refer to all subjects' maximum and minimum values.

2.3.3. In-depth Corner Entry Analysis

A data-mining approach was utilised to scrutinise the acquired signals, with no previous knowledge of the diversity of practices. While the analyses described previously were relative to multiple complete trials, the data mining approach was applied to single executions of a corner entry manoeuvre (shown in Figure 1a). The manoeuvre started in the middle of the previous straight to capture the braking pattern and ended slightly after the corner apex; considering a specific manoeuvre made it easier to compare different trials and interpret the results. The unsupervised technique used the Hierarchical Agglomerative Clustering (HAC) algorithm (Hastie et al., 2009). This algorithm clusters observations with high levels of similarity in the same cluster (intra-cluster homogeneity); it ensures that the clusters are as different as possible (inter-cluster heterogeneity). The bottom-up and hierarchical clustering process starts from individual observations, producing more prominent groups, including subgroups. The dendrogram is then cut at a user-chosen height to attain the desired partition. Dynamic Time Warping (DTW) (Senin, 2008) was used as a metric to determine the distance between two observations. In contrast, the distance between two clusters was measured using the single-linkage criterion, the minimum distance among cluster data points.

HAC was applied to identify trials showing similar behaviour and to detect patterns relating each cluster to different riders or instructions. Two clustering processes were executed: one investigating the motorcycle dynamics and another investigating the rider inputs:

- The **'Motorcycle Dynamics'** clustering considered the speed v, longitudinal acceleration a_x, and roll angle ϕ signals. Each signal's mean and standard deviation were used as features; for the roll signal, the maximum and minimum values were also considered.
- The **'Rider Inputs'** clustering considered the steering torque τ_{steer}, perpendicular torque $\tau_{\perp}$, foot-peg torque τ_{feet}, and saddle centre of pressure coordinates $\text{CoP}_{x,y}$ signals. The mean and standard deviation of each signal were used as features, except for the longitudinal position on the saddle for which the mean was not considered[11].

In the article, a symbol with an overline refers to its mean, while σ is the standard deviation.

3. Results

3.0.1. Familiarisation

Figure 5a shows the evolution of the g-g diagram during the three FR trials of one rider (S_3). The convex envelope corresponding to each sampling instant is shown; the colour shifts from dark blue to yellow as the rider covers the distance (840 m for the sum of three trials). Even in the third trial, the rider covered parts of the diagram whose acceleration levels were not reached previously.

The evolution of the area of the rider-capability envelope is shown for each subject as a function of the distance travelled as a dotted line in Figure 5b. Equation (2), computed with parameters A^* and s^* obtained through best-fit regression, is plotted as a solid line. The coefficient of determination was high for all subjects, ranging from $R^2 = 0.91$ for S_1 to $R^2 = 0.99$ for S_5. Subjects 3

[11] This choice was made as the mean longitudinal position on the saddle is influenced by the rider height, and only its standard deviation is linked to their behaviour.

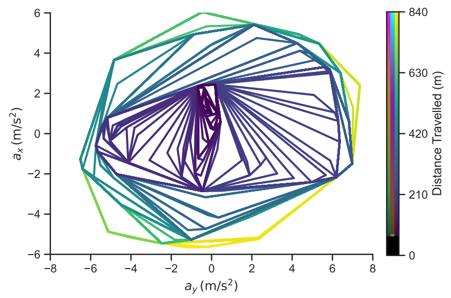

(a) Evolution of the capability envelope of Subject 3.

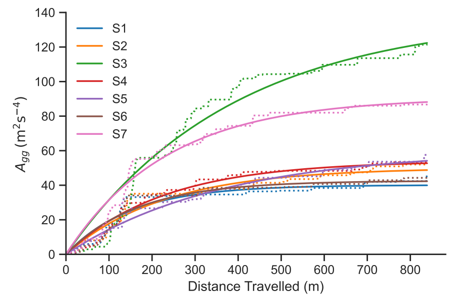

(b) Evolution of the area of the capability envelope of each subject. The effective evolution is shown as a dotted line and is approximated as a negative exponential (solid lines).

Figure 5: Familiarisation process described through the rider-capability envelope.

and 7 had a particularly high asymptotic area of the capability envelope, which spanned from $40.1\,\mathrm{m^2\,s^{-4}}$ ($\mathrm{S_1}$) to $138.0\,\mathrm{m^2\,s^{-4}}$ ($\mathrm{S_3}$). The distance constant s^* spanned from 151 m for $\mathrm{S_1}$ to 386 m for $\mathrm{S_3}$. The distance constant was positively correlated with the asymptotic area ($R = 0.72$): the riders who reached higher acceleration values tended to improve for longer. There was a strong positive correlation ($R = 0.90$) between the experience factor and the asymptotic area and a weaker one ($R = 0.49$) between experience and the distance constant. In addition to improving for longer, more expert riders improved quicker in the initial phase: the slope of Equation (2) at the origin, equal to A^*/s^*, had a 0.84 correlation with the experience factor. The correlation would have been even higher if considering 'time' as the independent variable, as more expert riders tended to ride faster, therefore covering the same distance in less time. Subject 5 was peculiar: he had the lowest slope at the origin, showing modest initial improvement; however, his capability envelope continued to expand along the trials, becoming the third largest at the end. Table 2 contains each subject's various metrics values. In particular, the 'Familiarisation' section shows each rider's coefficients related to the familiarisation process.

Table 2: Each subject's values of the metrics describing their riding style. The metrics are divided into four groups: those relative to the familiarisation process, to the g-g diagram, to the J-J diagram, and to experience and confidence.

	S_1	S_2	S_3	S_4	S_5	S_6	S_7	**Mean**	**SD**
Familiarisation									
A^* ($\mathrm{m^2\,s^{-4}}$)	40.09	50.02	138.01	54.07	60.16	42.56	90.69	**67.95**	**31.17**
s^* (m)	151.23	227.47	385.52	227.16	364.81	163.87	234.49	**250.65**	**91.12**
g-g Diagram									
$a_{x\max}$ ($\mathrm{m\,s^{-2}}$)	4.02	5.70	6.68	5.95	4.72	5.66	6.36	**5.58**	**0.92**
$a_{y\max}$ ($\mathrm{m\,s^{-2}}$)	7.65	6.62	7.35	6.58	6.78	7.56	6.76	**7.05**	**0.46**
m (-)	1.02	0.94	1.52	1.00	1.00	0.80	1.42	**1.10**	**0.26**
A ($\mathrm{m^2\,s^{-4}}$)	62.77	70.79	135.61	78.4	78.39	66.19	114.19	**84.6**	**28.70**
J-J Diagram									
$J_{x\min}$ ($\mathrm{m\,s^{-3}}$)	-17.39	-20.98	-41.59	-28.90	-25.12	-22.45	-29.30	**-26.53**	**7.89**
$J_{x\max}$ ($\mathrm{m\,s^{-3}}$)	15.16	15.13	29.23	19.36	17.17	14.43	17.16	**18.23**	**5.13**
$J_{y\max}$ ($\mathrm{m\,s^{-3}}$)	14.67	12.79	15.09	12.75	11.65	17.19	17.60	**14.54**	**2.28**
m (-)	1.30	1.26	1.17	0.92	0.97	1.15	1.27	**1.15**	**0.15**
A ($\mathrm{m^2\,s^{-6}}$)	275.13	298.49	552.62	299.19	277.55	283.77	386.20	**338.99**	**101.64**
Experience-Confidence									
expFactor (-)	0.26	0.00	0.74	0.17	0.21	0.15	0.60	**0.30**	**0.27**
$\overline{a_{xy}}$ ($\mathrm{m\,s^{-2}}$)	1.77	1.94	3.84	2.55	2.27	2.12	2.97	**2.50**	**0.71**
$\overline{\phi_{xy}}$ (rad)	0.27	0.25	0.30	0.26	0.27	0.27	0.30	**0.28**	**0.02**
$\overline{J_{xy}}$ ($\mathrm{m\,s^{-3}}$)	4.01	3.75	5.46	3.90	3.71	3.93	4.93	**4.24**	**0.68**
confFactor (-)	0.21	0.04	1.00	0.18	0.17	0.17	0.72	**0.36**	**0.36**

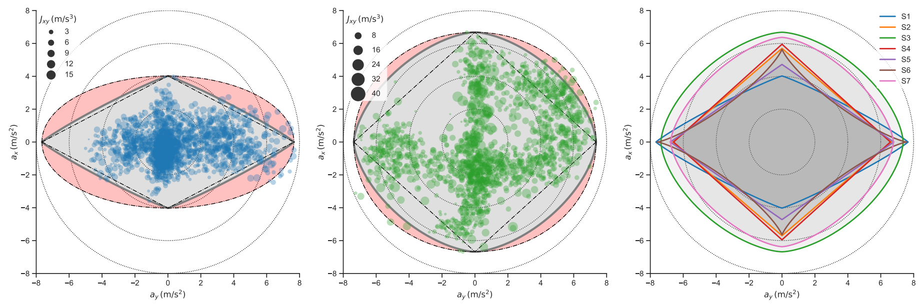

(a) Subject 1. (b) Subject 3. (c) Capability envelopes.

Figure 6: g-g diagrams and corresponding capability envelopes, relative to all trials. The area of each dot is proportional to the corresponding total jerk value.

3.0.2. Rider-Capability Envelope

Figures 6a and 6b compare the g-g diagrams of a rider with moderate experience (S_1) with that of an experienced rider (S_3). The area of each dot is proportional to the corresponding total jerk. The area of the capability envelope is shown in grey; two dash-dotted lines indicate the contour of the envelope with $m = 1$ (rhombus) and $m = 2$ (ellipse) as a reference: therefore, the red area indicates the potential area of the capability envelope lost due to using of combined dynamics less than what is theoretically possible, for the same maximum longitudinal and lateral acceleration values. Subject 1 reached the highest lateral acceleration values ($7.65\,\mathrm{m\,s^{-2}}$) when performing the left corners (positive lateral acceleration), but only modest longitudinal acceleration values ($\leq 4\,\mathrm{m\,s^{-2}}$). Combined dynamics was limited ($m = 1.02 \approx 1$): in practice, the rider summed the two acceleration components to assess the acceleration level. Subject 3 reached slightly lower lateral acceleration values ($7.35\,\mathrm{m\,s^{-2}}$) but much more intense levels of longitudinal acceleration ($6.68\,\mathrm{m\,s^{-2}}$), both in traction and in braking. Moreover, the rider used the combined dynamics much more, as indicated by the 1.52 value of his capability exponent. Consequently, the area lost due to a lower-than-possible use of the combined dynamics (in red) was limited.

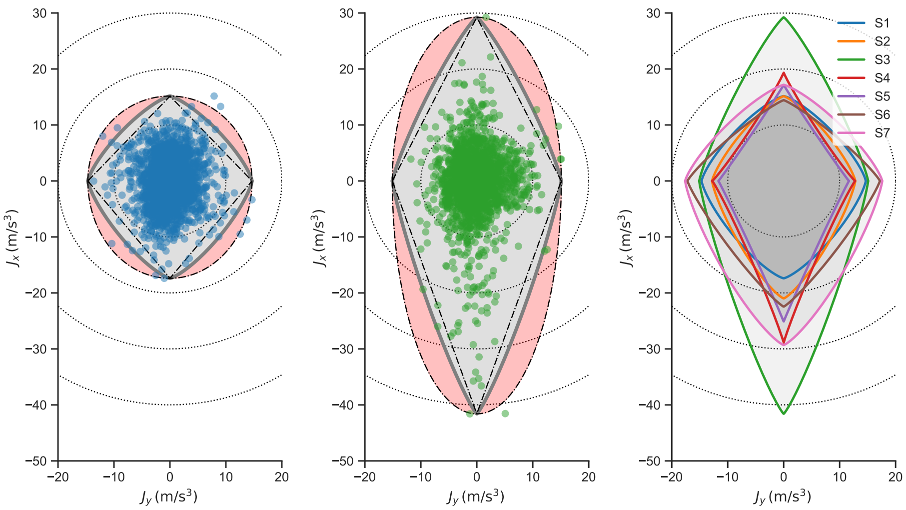

(a) Subject 1. (b) Subject 3. (c) Capability envelopes.

Figure 7: J-J diagrams and corresponding capability envelopes, relative to all trials.

Figure 6c compares the riders' capability envelope. Rider S_3 covered the widest area ($135.6\,\mathrm{m^2\,s^{-4}}$) of the g-g diagram, while S_1 was the most conservative ($62.8\,\mathrm{m^2\,s^{-4}}$). S_1 made the most modest use of longitudinal dynamics. S_6 severely limited the use of combined dynamics, producing the only concave capability envelope ($m = 0.80 < 1$). The properties of each rider's gg diagram are shown in the 'g-g Diagram' section of Table 2.

Figures 7a and 7b compare the previous subjects (S_1 and S_3) in terms of jerk. Similar maximum lateral acceleration values for these riders translated into analogous maximum lateral jerk values. As mentioned in Subsection 2.3, all riders reached higher values of the negative longitudinal jerk than positive ones: for example, Subject 3 reached $29.2\,\mathrm{m\,s^{-3}}$ in traction and $41.6\,\mathrm{m\,s^{-3}}$ when braking. All riders (Figure 7c) reached higher jerk values in the longitudinal direction than laterally. Compared to the g-g diagram, the exponent of the envelope was less variable: from 0.92 for S_4 to 1.30 for S_1. Values for all riders can be found in the section 'J-J Diagram' of Table 2.

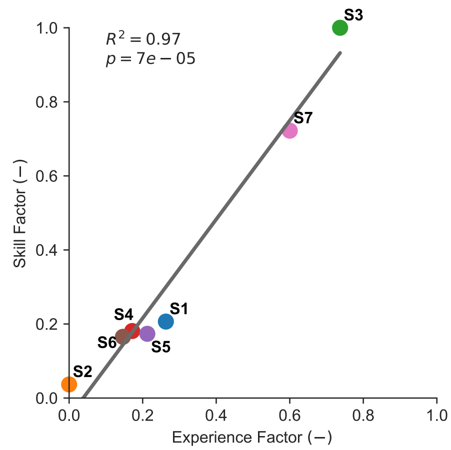

Figure 8: Regression showing the relationship between rider experience and confidence in exciting motorcycle dynamics.

Figure 8 plots the 'confidence factor' (Equation (9)) against the 'experience factor' (Equation (5)). Rider's confidence in exciting the motorcycle dynamics to a higher degree, in terms of total acceleration, total jerk and combined dynamics, was highly correlated ($R^2 = 0.97$ for the linear regression, $p = 7\text{e}{-5}$) with their experience, based on the years of licence and distance travelled in one year. The order of the seven riders sorted based on the experience factor was the same as the order based on the confidence factor, except for S_4 and S_5 which had almost identical skill factor values. S_3 had a 'confidence factor' equal to 1: he had the most extreme behaviour based on all the three metrics considered. Values for all riders can be found in the section 'Experience-Confidence' of Table 2.

3.1. In-depth Corner Entry Analysis

3.1.1. Motorcycle Dynamics

Figure 9 shows the results of applying the clustering to the dynamical features computed for the corner entry manoeuvre. The dendrogram (Figure 9a) was cut using a 0.39 threshold for the DTW distance, obtaining two clusters and two outliers.

Figure 9b shows the first two principal components, which explained 80% of

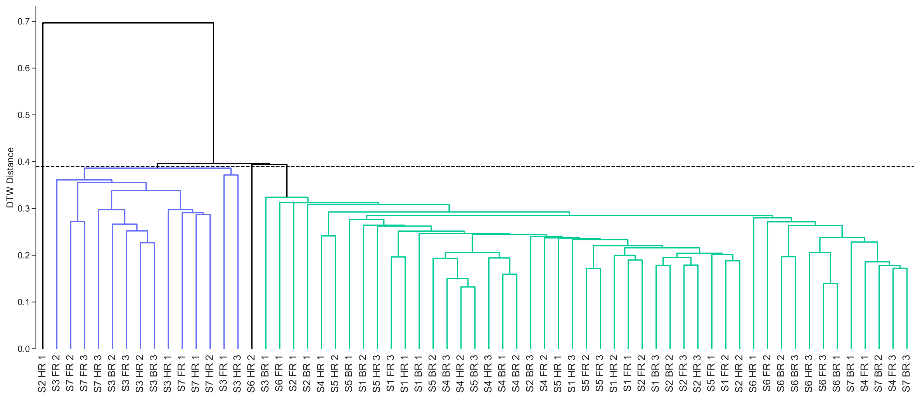

(a) Dendrogram, using Dynamic Time Warping (DTW) as the distance metric.

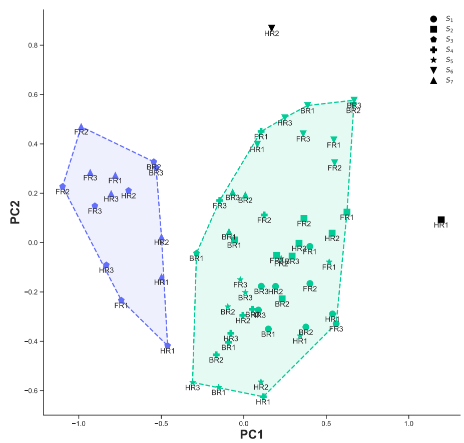

(b) The first two Principal Components: PC1 explains 55% of the variance, PC2 25%.

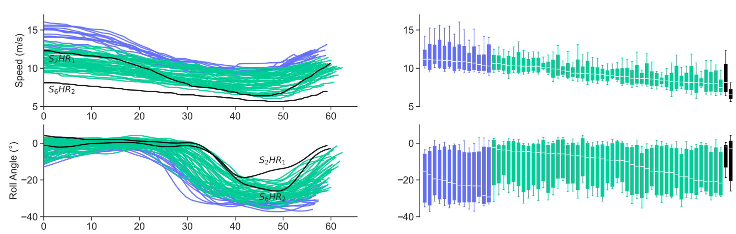

(c) Speed and roll angle signals. For each signal, the boxes relative to trials belonging to each cluster are sorted by descending median.

Figure 9: Results of the clustering algorithm applied to corner entry when using statistical properties of motorcycle dynamics signals as features. The High-Dynamics cluster is shown in blue, and the Low-Dynamics cluster in green. Outliers are shown in black.

the total variance of the dataset. In particular, the first principal component PC1 explained 55% of the variance and was sufficient to separate the two clusters: there was no overlap concerning the PC1 values. While PC1 described inter- and intra-cluster differences, PC2 only represented the difference among trials belonging to the same cluster. PCA loadings showed that PC1 was negatively correlated with the mean speed $\bar{v}$ and the roll angle standard deviation $\sigma(\phi)$ and positively correlated with the minimum roll angle $\phi_{\min}$ and its mean $\bar{\phi}$: this means travelling slower along the corner, producing a more modest average and maximum roll (as the roll is negative in a leftward corner). Overall, high PC1 values indicated less intense lateral dynamics. Trials belonging to the blue cluster had negative PC1 values; this cluster was named High-Dynamics (HD). The green cluster had more positive PC1 values; therefore, it was named Low-Dynamics (LD). PC2, instead, was positively correlated with $\sigma(v)$, $\phi_{\max}$, and $\sigma(a_x)$, and was negatively correlated with $\bar{a}_x$: trials in the upper part of Figure 9a had a more variable speed, which decreased throughout the manoeuvre (negative $\bar{a}_x$) with a highly variable longitudinal acceleration (higher $\sigma(a_x)$). High PC2 values indicated more intense longitudinal dynamics: the rider approached the corner at a relatively high speed and had to brake more intensely and for longer. As a leftward roll angle is negative, having a more positive $\phi_{\max}$ meant the rider widened the trajectory on corner entry by initially leaning to the right. One outlier (S_2HR_1) had an abnormally high PC1 value, travelling the corner at a very modest speed; the other (S_6HR_2) stood out compared to the Low-Dynamics trials for a peculiarly high PC2 value, indicating intense braking and high speed differentials.

These results, relative to the statistical features computed from the measured signals, were confirmed by the signals themselves. The speed and roll angle (Figure 9c) were plotted against the distance travelled[12] along the corner, and their statistical properties are shown through box plots. The higher speed of the

[12]The distance travelled along the corner differed slightly between different trials due to the trajectory variability.

trials belonging to the HD cluster was noticeable, with minimal overlap with the LD cluster, especially at the beginning and at the end of the manoeuvre. In the High-Dynamics cluster, the speed variation was more evident: as riders approached the corner faster, they tended to brake more. The speed reached its minimum around 5 m earlier than for the Low-Dynamics cluster, with earlier throttle use after the apex. There are some HD trials whose minimum speed was higher than the maximum speed reached in some LD trials. The S_2HR_1 trial was characterised by an unusually low speed, coherently with its high PC1 value: the maximum speed reached was lower than the minimum speed of most LD trials. The S_6HR_2 trial was characterised by a significant speed reduction from the beginning of the manoeuvre to the apex, as predicted by its high PC2 value. The higher speed of the trials belonging to the HD cluster produced higher roll angle values: the maximum was higher and was reached sooner, magnifying roll rate and roll acceleration compared to the LD trials. The roll angle was also maintained longer towards the exit of the curve, despite opening the throttle sooner: this indicated higher use of the combined dynamics. The very modest speed of the S_2HR_1 trial reflected on the low roll angle values ($<20°$).

Table 3 shows how the different riders and instructions were distributed between the clusters. Subject S_3 was most often in the HD cluster, with just one trial (his first BR trial) classified as LD. He was followed by S_7, whose FR and HR trials were classified as HD, and his BR trials as LD. Therefore, Subjects 3 and 7 had the confidence to get closer to the grip limits, but this was lessened when instructed to ride using their body. No other rider had a run classified as HD; two of them (S_2 and S_6) produced outliers. The BR instruction led to significantly fewer HD trials than others (two for BR, compared to six for FR and HR); HR was the only instruction that produced outliers.

3.1.2. Rider Inputs Analysis

Focus on S_7. As the trials of Subject 7, a professional trainer of military trainers, showed the most meaningful and repeatable difference based on the instruction given, the clustering on the riding inputs was first conducted considering

Table 3: The number of runs in each cluster (High-Dynamics, Low-Dynamics) and of outliers, for each subject S_i and instruction (Free-Riding, Handlebar-Riding, Body-Riding), when using the statistical properties of motorcycle dynamics signals as features. The distribution of the runs among the three groups is shown for each row as a percentage inside brackets.

	Cluster		
	HD	LD	Outliers
S_1	0 (0%)	9 (100%)	0 (0%)
S_2	0 (0%)	8 (89%)	1 (11%)
S_3	8 (89%)	1 (11%)	0 (0%)
S_4	0 (0%)	9 (100%)	0 (0%)
S_5	0 (0%)	9 (100%)	0 (0%)
S_6	0 (0%)	8 (89%)	1 (11%)
S_7	6 (67%)	3 (33%)	0 (0%)
FR	6 (29%)	15 (71%)	0 (0%)
HR	6 (29%)	13 (62%)	2 (10%)
BR	2 (10%)	19 (90%)	0 (0%)
Total	**14 (22%)**	**47 (75%)**	**2 (3%)**

his trials only.

As the trials considered just one rider, the large rider-dependent trials variability was removed; consequently, the first two principal components accounted for a significant portion (78%) of the variance. The remaining variability should then be described by the instruction and familiarisation process, mainly in the case of the FR trials, as they were conducted first.

The resulting dendrogram is shown in Figure 10a. Cutting the dendrogram at a 0.60 DTW threshold produced three clusters and one outlier. The first two Free Riding trials were the first trials to merge; then, the third FR trial joined the same cluster (in cyan, named 'Free Riding', or FR). After that, the two closest groups were the first two BR trials, which were joined by the third BR trial to form the pink cluster (named 'Body Riding', or BR). The first two HR trials belonged to the same cluster (in orange, named 'Handlebar Riding', or HR), whose intra-cluster similarity was lower than that of the other clusters. The FR and HR clusters merged; the resulting group was about as similar to the remaining HR trial as the BR cluster. Each cluster contained trials relative to a specific instruction.

The time signals were then investigated, and their statistical properties summarised through box plots (Figure 10b). All three FR trials presented a rapid steering torque increase on corner entry and high peak values. The HR and BR showed reduced use of the steering torque. The rider used higher steering torque inputs (Around 50% higher $\overline{\tau_{\text{steer}}}$ and $\sigma(\tau_{\text{steer}})$) when receiving no specific riding instruction.

BR presented a much lower use of the perpendicular torque as well. Peculiarly, in the HR cluster, the perpendicular torque grew very quickly, even more than for the FR cluster, although the steering torque was far smaller. FR instruction led to more intense actions on the handlebar, the opposite of the BR instruction. Following the HR instruction, actions were intense only in the direction perpendicular to the steering axis: the rider used the handlebar to make the motorcycle tilt.

Concerning the use of the foot-pegs, trials in the HR cluster showed minimal

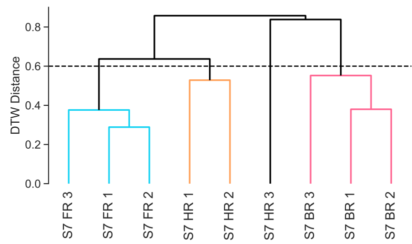

(a) Dendrogram, using Dynamic Time Warping (DTW) as the distance metric.

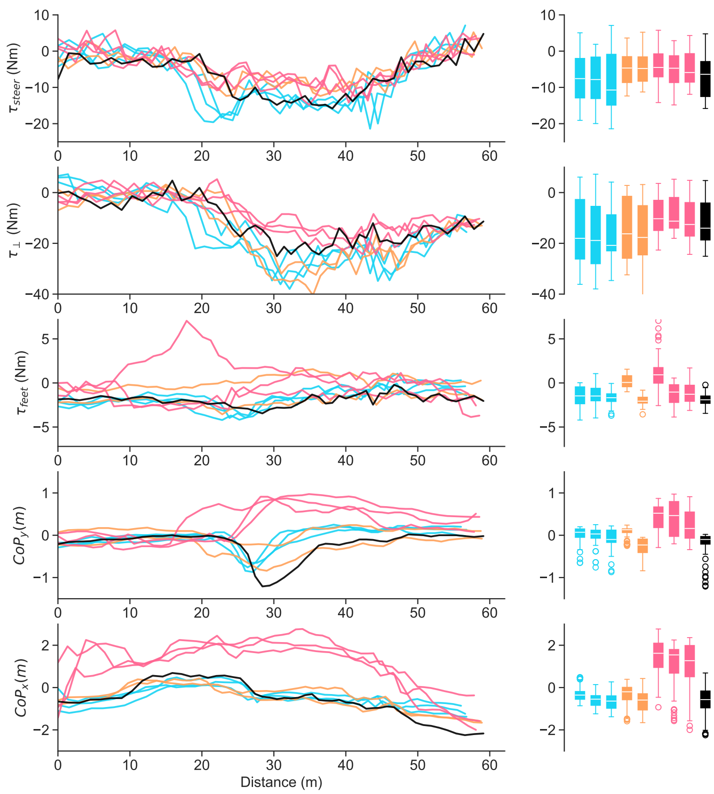

(b) Rider input signals. For each signal, the boxes relative to trials belonging to each cluster are sorted by descending median.

Figure 10: Results of the clustering algorithm applied to corner entry by Subject 7 when using statistical properties of rider input signals as features. The Free-Riding cluster is shown in cyan, the Handlebar-Riding cluster in orange, and the Body-Riding cluster in pink. Outliers are shown in black.

τ_{feet} variation through the trial. In the FR trial, a small negative torque (in the direction of the motorcycle lean) was generated when the rider moved to the right on the saddle. In the BR trials, the use of the foot-pegs was intense, particularly in the case of one trial: again, τ_{feet} and CoP_y had the same signs, but differently from the other trials they were positive.

The difference among clusters was apparent regarding lateral displacement over the saddle. In the FR trials, the rider sat centred on the saddle at the beginning and end of the manoeuvre, and he moved to the right (towards the outside of the corner) in the corner entry phase. This repeated to a lower degree in the HR cluster. For the BR cluster, the behaviour was radically different: the rider moved towards the left on the saddle and kept this position throughout the remainder of the manoeuvre.

The characteristics of the BR cluster were peculiar also concerning the longitudinal displacement: the rider moved significantly towards the front of the motorcycle starting from the initial braking phase, while he slid towards the back when starting to use the throttle; the rider in the BR trials, therefore, could be modelled as a mass-spring system with much lower stiffness. As the movement in both directions was intense, the rider interpreted the BR instruction as 'to move significantly over the saddle'.

The outlier (S_7HR_3) showed analogies with HR and FR trials but differentiated mainly concerning the use of handlebar torques. In this trial, τ_{steer} was intermediate between FR and HR trials, while $\tau_{\perp}$ was lower than for both. The movement over the saddle was analogous but higher than that of the FR trials.

All Subjects. After analysing the trials by Subject 7, the clustering was repeated considering all the riders so that the placement of S_7's trials in the various clusters could be used to understand the meaning of each. Figure 11 shows the dendrogram obtained; a 0.35 DTW distance threshold was used to cut it, obtaining five clusters and several (11) outliers, indicating significant variability in the inputs given to the vehicle. Three clusters (indicated in yellow, green and red) contained few trials, all relative to a specific rider-instruction combination.

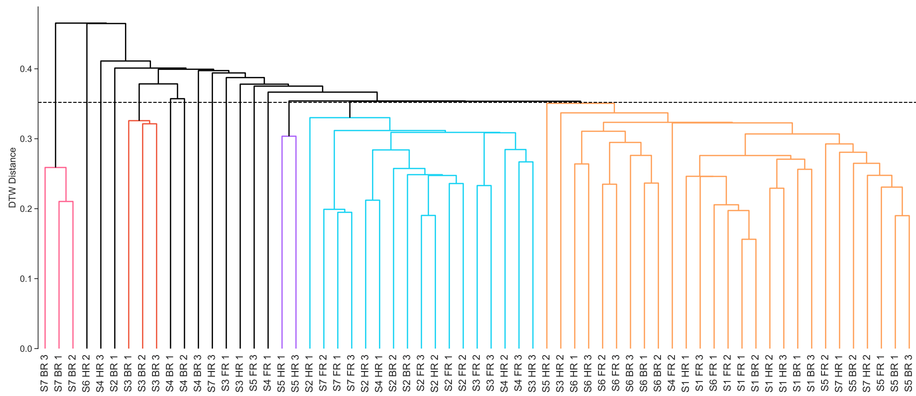

Figure 11: Dendrogram showing the clustering algorithm results when using the statistical properties of rider input signals as features.

The other two clusters contained a much higher number of trials; therefore, they were more diverse in terms of the subjects and instructions represented; in fact, the roots of the clusters were placed slightly higher than for the three smaller clusters. The five signals considered were uncorrelated: except for the correlation between the steering torque and the perpendicular torque, which are produced by the same action (the forces applied on the handlebar), the strongest correlation among other signals was just -0.19 (the one between $\tau_\perp$ and τ_{feet}). The correlation between statistical features was modest as well; the highest correlation between any two features relative to different signals was 0.37, between $\sigma(\text{CoP}_x)$ and $\sigma(\text{CoP}_y)$: for a given trial, the rider tended to move more over the saddle in one direction when there was higher movement in the other direction. The correlation between the time signals and that between the statistical features was lower compared to what was obtained considering only S_7, as expected.

Clusters are numbered from left to right in the dendrogram. Their properties are derived by looking where the previously discussed clusters for S_7 are placed among them and by looking at the statistical properties of each (shown in Table 4).

- Cluster C_1 coincided with the BR cluster described previously for S_7. In

Table 4: Values of the statistical features computed from the rider input signals for each cluster. For the mean values, the cell is red if the value is negative, white if it's null, and blue if it's positive. For the standard deviation values, the cell colour goes from white if the value is zero to dark grey for the highest value.

	C1	C2	C3	C4	C5	Outliers	Weighted Mean
mean(τ_steer)	-4.64	-4.14	-3.48	-7.51	-3.89	-5.93	-5.29
σ(τ_steer)	4.60	3.31	3.99	5.12	4.47	4.91	4.66
mean(τ_perp)	-9.58	-16.00	-24.18	-12.42	-15.02	-12.05	-13.83
σ(τ_perp)	7.33	8.73	16.16	11.06	9.95	11.61	10.58
mean(τ_feet)	-0.38	-1.02	4.58	-0.33	0.01	0.78	0.14
σ(τ_feet)	1.44	0.56	1.41	1.27	0.96	1.88	1.24
mean(CoPy)	0.34	0.97	-0.57	0.03	-0.18	0.11	0.00
σ(CoPy)	0.38	0.54	0.12	0.15	0.15	0.37	0.22
σ(CoPx)	1.11	0.54	0.40	0.34	0.29	0.44	0.39

these trials, the rider minimised the perpendicular torque (smallest mean and standard deviation). The rider moved significantly longitudinally on the saddle (maximum $\sigma(\mathrm{CoP}_x)$ value) and quite a lot laterally as well (second highest $\sigma(\mathrm{CoP}_y)$ value), varying the footpegs torque in the process (maximum $\sigma(\tau_{\mathrm{feet}})$ value). These evidences attest that S_7 interpreted the BR instruction as 'Apply minimal torque on the handlebar; move the buttocks and use the foot-pegs to lean the motorcycle'.

- Cluster C_2 contained the three BR trials of S_3. He used the steering torque minimally (lowest standard deviation and modest mean) and the perpendicular torque modestly. The foot-pegs torque was negative on average, making the motorcycle roll more, and it had the lowest standard deviation. The rider was on the left side of the saddle on average (highest and positive $\overline{\mathrm{CoP}_y}$), moving significantly (highest $\sigma(\mathrm{CoP}_y)$). S_3 interpreted the BR instruction as 'Do not use the handlebar to make the motorcycle lean; move the buttocks and use the foot-pegs for that'.

- Cluster C_3 contained two HR trials by S_5. The use of τ_{steer} was minimal, while $\tau_\perp$ was by far the highest as both mean and standard deviation. This cluster was the only one with a clearly negative $\overline{\mathrm{CoP}_y}$ value, and it also had the lowest $\sigma(\mathrm{CoP}_y)$: the rider remained on the right side of the saddle, and moved minimally. S_5 interpreted the 'HR' instruction as 'use the handlebar mostly to lean the motorcycle and do not move laterally over the saddle'. $\overline{\tau_{\text{feet}}}$ was the highest by far and positive: the rider used the foot-pegs to straighten the motorcycle, and this action was probably linked to his position over the saddle.

- Cluster C_4 contained eight trials of S_2, three of S_3, three of S_4, and the three FR trials by S_7. It contained four riders and multiple instructions, mainly FR and HR. The cluster was relative to intense use of the steering torque: $\overline{\tau_{\text{steer}}}$ and $\sigma\left(\tau_{\text{steer}}\right)$ were highest. Movement over the saddle was extremely limited in both directions (low $\sigma(\text{CoP}_{x,y})$ values), as the rider sat on the centerplane on average ($\overline{\text{CoP}_y} \approx 0$). The FR cluster described previously for S_7 is a subset of C_4 trials $\in$ C_4 are similar to how S_7 rode when subject to the FR instruction, applying high steering torque and a small, negative torque through the foot-pegs, with limited movement over the saddle.

- Cluster C_5 contained 26 trials belonging to six different riders and all the riding instructions, about equally: 9 FR trials, 8 HR trials and 9 BR trials. In particular, it contained all the trials by S_1. Consequently, the trial was relatively diverse; however, common characteristics emerged. Longitudinal movement over the saddle was the lowest, and the lateral movement was also very low. On average, the torque applied through the foot-pegs was null. The cluster contained trials which did not show extreme behaviour concerning the other signals. HR $\subset$ C_5: trials $\in$ C_5 show analogies to how S_7 rode when subject to the HR instruction: much higher $\tau_{\perp}$ than τ_{steer}, minimal movement over the saddle and small foot-pegs torque.

Table 5 shows the distribution among the clusters of the trials by each rider or instruction. Three categories of riders emerge concerning whether they followed the instructions given:

Table 5: The number of runs in each cluster and of outliers, for each subject S_i and instruction (Free-Riding, Handlebar-Riding, Body-Riding), when using the statistical properties of rider input signals as features. The distribution of the runs among the six groups is shown for each row as a percentage inside brackets.

	Cluster					
	C_1	C_2	C_3	C_4	C_5	Outliers
S_1	0 (0%)	0 (0%)	0 (0%)	0 (0%)	9 (100%)	0 (0%)
S_2	0 (0%)	0 (0%)	0 (0%)	8 (89%)	0 (0%)	1 (11%)
S_3	0 (0%)	3 (33%)	0 (0%)	3 (33%)	1 (11%)	2 (22%)
S_4	0 (0%)	0 (0%)	0 (0%)	3 (33%)	1 (11%)	5 (56%)
S_5	0 (0%)	0 (0%)	2 (22%)	0 (0%)	6 (67%)	1 (11%)
S_6	0 (0%)	0 (0%)	0 (0%)	0 (0%)	8 (89%)	1 (11%)
S_7	2 (22%)	0 (0%)	0 (0%)	3 (33%)	2 (22%)	1 (11%)
FR	0 (0%)	0 (0%)	0 (0%)	9 (43%)	9 (43%)	3 (14%)
HR	0 (0%)	0 (0%)	2 (10%)	6 (29%)	8 (38%)	5 (24%)
BR	3 (14%)	3 (14%)	0 (0%)	2 (10%)	9 (43%)	4 (19%)
Total	**3 (5%)**	**3 (5%)**	**2 (3%)**	**17 (26%)**	**26 (41%)**	**12 (19%)**

- Subjects $S_{1,2,6}$ did not follow the instructions, as all the trials which were not outliers belonged to the same cluster, independent of the instruction. These clusters were C_5 for S_1, C_4 for S_2, and C_5 for S_1; therefore, S_1 and S_6 also had a similar riding style. The familiarisation process did not influence their riding inputs, as well.

- Subjects $S_{3,7}$, the most experienced ones, followed the instructions. All the BR instructions by S_3, and only those, belonged to a specific cluster, highlighting a different behaviour compared to his HR and FR trials. S_7 had its trials classified in a different cluster for each instruction.

- Subjects $S_{4,5}$ had trials belonging to different clusters; however, there was not a clear relationship between instruction and consequent cluster: so their behaviour changed in a mostly chaotic way. In particular, S_4 produced five outliers: his riding style was inconsistent and not repeatable.

The riding style preference stated <u>before</u> the test (handlebar vs body, in Table 1) was compared with the clustering results. All trials by $S_1 \in C_5$ which is relative to high perpendicular torque and minimal movement over the saddle: this is coherent with the higher score the rider assigned to 'riding through the handlebar' compared to 'riding through the body' (8.0 vs 5.6). Eight trials by $S_2 \in C_4$ which is relative to high steering torque values while not moving on the saddle: also S_2 gave a clear preference to riding through the handlebar, coherently with his behaviour. His only outlier is a BR trial. S_3's BR trials are in a separate cluster: this instruction led him to ride differently than when subject to the FR instruction, which is coherent with his stated preference about riding using the handlebar. S_4 produced five outliers, which included his very first trial, probably due to the effect of familiarisation, and all his BR trials; before the test, he stated equal preferences concerning riding using the handlebar and using the body, but after the test, he expressed an appreciation for the HR instruction. S_5 was the only rider to state a clear preference concerning riding with the body (8.4 vs 5.2): in fact, the BR instruction was the only one that produced trials belonging to the same cluster. S_6 didn't have trials belonging to different groups as the instruction changed: his preference was about the same concerning riding using mainly the handlebars or the body (6.5 vs 6.7), and this lack of preference might have influenced his lack of behavioural change.

4. Discussion

Overall, the results showed appreciable differences between the riders, significantly influenced by experience. For a given rider, rider behaviour evolved as the familiarisation process occurred. For most riders, the instruction imparted clearly influenced behaviour, especially concerning the inputs used.

The familiarisation analysis showed that all the riders tended to explore additional portions of the g-g diagram along the trials. As was hypothesised, the growth of its area as a function of the travelled distance was excellently described by a negative exponential (lowest coefficient of determination equal to 0.91). The expansion of the capability envelope continued in the subsequent familiarisation trials, even though the riders were never told to ride faster as they gathered experience: the process happened naturally. A significant variability emerged among riders regarding the asymptotic area, for which experience was a precise predictor, and the distance travelled before reaching the asymptote. The fit was worse in the first 100 m, as the rider started from a standstill on the initial straight: as such, the first points on the g-g diagram were all located on the upper part. Therefore, even if the longitudinal acceleration was significant, the envelope area was small; it was only in correspondence to the first corner that the rider explored a different part of the diagram, producing an abrupt area increase.

Concerning the estimated capability envelope of each rider, some patterns emerged. All riders reached higher acceleration values in the lateral than the longitudinal direction. The inter-rider difference was surprisingly modest in terms of lateral acceleration ($1.07\,\mathrm{m\,s^{-2}}$ difference between the lowest and highest $a_{y\max}$ values). It was more significant in terms of longitudinal acceleration ($a_{x\max}$ ranged from $4.02\,\mathrm{m\,s^{-2}}$ to $6.68\,\mathrm{m\,s^{-2}}$). Each rider had similar longitudinal acceleration levels when using the throttle compared to braking. The difference in the longitudinal dynamics concerning jerk was even higher, particularly when braking: the highest $J_{x\min}$ value was around 2.5 times the lowest. The high variability in the negative jerk values confirms the results of previous research on the braking patterns of riders with various skill levels (Huertas-Leyva et al., 2019). Concerning the riders who reached the highest negative jerk values, the high jerk was produced by quickly transitioning from high throttle use to strong braking, producing a significant and quick longitudinal acceleration differential. Opposite to the evidence concerning the acceleration values, the lateral jerk was more modest than the longitudinal one. Although there was a clear indication that more experienced riders tended to excite the combined dynamics more, the variability of the jerk capability exponent was more modest and less correlated with experience. A higher frequency of the feedforward control, required for minimising travel time given friction conditions or minimising the grip required for a given travel time (Limebeer and Massaro, 2018), inherently produces higher jerk values. A more intense feedback action, which might be linked to a less stable vehicle or a more erratic rider (Lot and Sadauckas, 2021), can produce higher jerk levels, too. Further research should differentiate between the two, potentially providing suggestions to improve training programs. To summarise, more expert riders used a more intense braking action, which was applied more abruptly and continued well into the corner. Experience predicted very well ($p = 7\text{e}{-5}$) the intensity of the riding dynamics in terms of acceleration magnitude and combination and jerk magnitude. The J-J diagram, proposed in this work, was useful for comparing riders in terms of jerk values in addition to acceleration. It should be noted that jerk, and in particular the measured peaks, are particularly dependent on the specific motorcycle used (e.g. suspension damping) and the filtering performed on the computed jerk[13]. However, this does not impact the comparison of trials performed using

[13]In this work, jerk was computed as the central finite difference of the acceleration signal (sampled at 10 Hz), then filtered through a Savitzky–Golay filter with a cubic polynomial and

the same hardware and software, like in the case of the present study or for an instrumented motorcycle employed by a riding school. Other studies have shown that rider behaviour can repeatedly differ between right and left-hand corners (Magiera et al., 2016); future work could extend the asymmetry of the ellipse to the lateral direction, too. In naturalistic riding sessions, elements like roundabouts, which are always travelled in the same direction, might explicitly induce this phenomenon.

The HAC algorithm classified the different trials concerning the corner entry manoeuvre, highlighting the characteristics of the various riders and each one's behaviour following a specific instruction. The 'Motorcycle Dynamics' clustering produced two groups, distinguished by the intensity of the corresponding dynamics. The 'High-Dynamics' (HD) cluster only contained trials by the two most expert riders: therefore, rider experience was a more impactful factor than the riding instruction concerning the intensity of the dynamics observed. Still, the Body Riding (BR) instruction could (always in case of S_7, in the first attempt in the case of S_3) move a subject's trial from the HD cluster to the Low-Dynamics (LD) one. Notably, the opposite effect was never observed: in no case did the BR instruction move a rider from cluster LD to cluster HD. The principal components projection proved useful in understanding the intra- and inter-cluster differences. Each component described one distinct aspect of the motorcycle response: lateral dynamics in the case of PC1, mainly the mean lateral acceleration or roll angle, which for a given trajectory is linked to the mean speed, and the longitudinal dynamics in the case of PC2, in terms of mean and variation of the longitudinal acceleration. The HD trials were also characterised by more intense use of the combined dynamics. The HD cluster had a lower variance in the speed signal across different trials (Figure 9c) compared to the LD cluster: this is partly due to fewer trials (14 vs 47). However, there could be an additional explanation: as a rider reduces the manoeuvre execution time, they will, on average, remain closer to the edge of the friction envelope;

a 5-points window size.

in doing so, the set of acceleration signals resulting in a given travelling time reduces. The limit case is the 'optimal manoeuvre', consisting of a unique combination of inputs that leads to the theoretical minimum time. On the contrary, when travelling slower on average, a rider can complete the manoeuvre in a given time using various combinations of longitudinal and lateral acceleration profiles: one could say that 'there are many ways to ride slowly and fewer ways to ride quickly'. Another factor could be that the HD consisted of trials by S_3 and S_7 only, who are very experienced riders that probably found it easier to have a repeatable behaviour. Just two trials (3%) were outliers: in terms of motorcycle dynamics, most attempts could be described as a variation of a more general case. The S_2HR_1 trial was abnormally slow; however, no instabilities or events of interest emerged when checking the video footage. For S_2, the HR instruction followed the FR trials, so the HR_1 trial was the first one in which a specific riding instruction was given: this probably caused some discomfort to S_2, which was the only rider still getting their licence at the time of the test. The other outlier (S_6HR_2) was produced by the rider with the shortest licence age (one year).

On the other hand, the 'Rider Inputs' clustering showed high variability concerning the possible input combinations a rider can use to enter a corner. Some riders followed the instructions, changing their behaviour based on their instruction interpretation. For example, S_3 and S_7 both followed the BR instruction but did so in slightly different ways, both coherent with the concept of 'riding using the body': the instruction was deliberately generic, leading to this result. Others did not follow the instructions to the same extent: a subset of riders did not change behaviour based on the instruction, and others did chaotically such that the instruction only explained a part of riding style variation. A much higher number of clusters (five) and outliers (eleven) resulted when classifying the trials based on the inputs given instead of the consequent motorcycle response. All the measured inputs were relative to lateral dynamics, for which the steering torque τ_{steer} is the primary input; instead, the other actions, like pushing the footpegs or moving laterally over the saddle, have a modest effect on the motorcycle response and are mainly linked to psychology and comfort (Weir and Zellner, 1978). In fact, S_7, who has high consciousness and preparation being a professional trainer of trainers, expressed a strong preference concerning the use of the handlebar and counter-steering (9.2 and 9.3, respectively), and very low scores about pushing against the footpegs (1.3) and the tank (3.4). In his case, the instruction dictated the inputs he used, with solid repeatability. The clear instruction-dependent behaviour difference manifested in each one of the time signals considered in the clustering. Identifying the meaning of each cluster using the proposed approach was relatively easy, despite the high number of subjects, instructions, trials, repetitions, and features used. The statistics of each feature cluster showed the peculiar aspects of each cluster. Even though not all riders followed the instructions, their behaviour was overall in line with the preference given before the test; when this was not true, the rider corrected their opinion in the post-test questionnaire. In all trials, the rider counter-steered and applied a leaning torque towards the fall ($\tau_{\text{steer}}, \tau_{\perp} < 0$ in the leftward corner): this is coherent with the results by Wilson-Jones (Wilson-Jones, 1951). Notably, even though counter-steering was always clearly present as it's an unavoidable phenomenon, S_5 stated in the questionnaire that they make limited use of it: this lower consciousness might induce the rider to apply a steering torque in the wrong direction during emergencies, greatly limiting the probability of avoiding the obstacle (Nugent et al., 2019). The clustering process considered either the rider inputs or the corresponding motorcycle response, while the link between the two was only considered indirectly: in the future, the relationship between the two should be assessed explicitly, for example, by applying the HAC to the union of the two sets of features proposed in this work. Additionally, statistics relative to the throttle position and brake pressure signals (not recorded during the experiment) should be added as features to complement the inputs related to trajectory control to those linked to managing the speed. In particular, a given deceleration can be achieved through different front-rear brake pressure combinations, possibly linked to experience and skill.

This work investigated riding preferences and style concerning the inputs used and the corresponding motorcycle dynamics for a diverse set of riders and evaluated the impact of familiarisation and the instruction given on their behaviour. A strong correlation was found between the rider's experience and several traits, such as the level of acceleration and jerk used and the usage of combined dynamics, and suggests conducting additional research to draw more general conclusions. Limitations consist of the modest length of each trial, which was conducted in a controlled environment: future work should extend the approach to a longer naturalistic ride on open roads to assess riding style and preferences in the real world, as the road width and absence of traffic could have impacted the rider behaviour. On the other hand, conducting trials following a pre-defined path in a controlled environment removed several external factors, like traffic or the properties of the road chosen, making the trials, whose statistics are compared, likewise. Moreover, the sophisticated instrumentation was not invasive and only a few sensors were visible: as the subjects did not know which quantities were measured, their behaviour was influenced less by the measurement apparatus. The work considered a small sample ($N = 7$) of riders, and only one of them was a professional trainer, even though one can expect professional riders to have less variable behaviour due to the training; therefore, the generalisability of the values obtained concerning the various metrics is limited. However, most other studies that compare the behaviour of different subjects using sensors consider a lower or analogous number of participants.[14] Yet, inter-rider variability was significant, and the correlation with experience was statistically significant. The main contribution of this work is methodological: the approach and metrics proposed can be employed for more extensive panels of participants. The work proposed an automatic approach to identify several metrics related to riding preferences and capability: these could be used as features for the HAC algorithm to classify riders based on their macroscopic behaviour, for example, concerning using combined dynamics or the familiarisa-

[14] $N = 2$ (Magiera et al., 2016), $N = 3$ Biral et al. (2005), $N = 7$ (Diop et al., 2023), $N = 8$ (Diop et al., 2020), $N = 12$ (Will et al., 2020).

tion process. The approach could aid researchers in characterising rider models relative to different skill levels or even corresponding to a real rider. Lastly, comparing the signals to the corresponding cluster's statistical features might help detect instabilities or the cause of a crash.

5. Conclusions

This work investigated the difference in riding style, preference, capability, and willingness to excite the motorcycle dynamics of a diverse set of riders. A significant inter-rider difference was found concerning the riding inputs employed and the corresponding motorcycle response. The effect of the riding instruction received, the rider's stated preference, and the familiarisation process was investigated. The novelty consists in the reproducibility of the objective and automatic approach proposed and the focus on the impact of experience and stated preference on behaviour, including the inputs used. This approach, which worked well even in such a repetitive riding condition, discriminating well between subjects doing the same manoeuvre, has considerable application potential for analysing naturalistic data, where the differences between riders will be even more apparent. The diversity of riding practices, and the minimal effect of some inputs used, warrant a revision of training and retraining practices to direct behaviour towards improved safety and make riders aware of the inputs that determine much of the PTW response, such as steering torque. Their consequences in terms of comfort should also be investigated in more detail. The most safety-effective riding styles, i.e. those that allow for greater manoeuvrability, should be identified and taught; in terms of capabilities, one could aim to raise the level of each trainee. The approach proposed could make research on rider behaviour more straightforward and objective and allow trainers to track the progress made by the trainees easily.

CRediT authorship contribution statement

Mirco Bartolozzi: Conceptualization, Methodology, Software, Formal analysis, Investigation, Data Curation, Writing - Original Draft, Visualization. **Abderrahmane Boubezoul:** Conceptualization, Methodology, Software, Formal analysis, Investigation, Data Curation, Writing - Review & Editing, Visualization. **Samir Bouaziz:** Investigation, Resources, Data Curation. **Giovanni Savino:** Writing - Review & Editing, Supervision. **Stéphane Espié:** Investigation, Resources, Writing - Review & Editing, Supervision, Project administration, Funding acquisition.

Declaration of Competing Interest

The authors declare that they have no known competing financial interests or personal relationships that could have appeared to influence the work reported in this paper.

Acknowledgement

The authors thank Le Centre national de formation à la sécurité routière-Fontainebleau for contributing to the experimentation. We thank Flavien Delghier for his contribution to the instrumentation.

Funding

This research received a grant from the Agence Nationale de la Recherche (ANR) funding agency for the VIROLO++ project, grant number: ANR-15-CE22-0008.

Data availability

Data will be made available on request.

References

M. Abreu de Souza, H. Gamba, and H. Pedrini. Multi-Modality Imaging: Applications and Computational Techniques. Springer, 2018. ISBN 9783319989747, 331998974X. doi: 10.1007/978-3-319-98974-7.

ACEM. MAIDS. Final Report. Technical Report 2, European Association of Motorcycle Manufacturers, 2008.

M. Bartolozzi, A. Boubezoul, S. Bouaziz, G. Savino, and S. Espié. Data-driven methodology for the investigation of riding dynamics: A motorcycle case study. IEEE Transactions on Intelligent Transportation Systems, 24(9): 10224–10237, 2023a. doi: 10.1109/TITS.2023.3271790.

M. Bartolozzi, A. Niccolai, C. Lucci, and G. Savino. Motorcycle emergency steering assistance: A systematic approach from system definition to benefit estimation and exploratory field testing. Accident Analysis & Prevention, 2023b. ISSN 0001-4575. doi: 10.1016/j.aap.2023.107116.

M. Bartolozzi, G. Savino, and M. Pierini. Motorcycle steering torque estimation using a simplified front assembly model: experimental validation and manoeuvrability implications. Vehicle System Dynamics, 2023c. doi: 10.1080/00423114.2023.2194542.

L. Beck, A. Dellinger, and M. O'Neil. Motor vehicle crash injury rates by mode of travel, united states: Using exposure-based methods to quantify differences. American journal of epidemiology, 166:212–8, 08 2007. doi: 10.1093/aje/kwm064.

F. Biral, M. Da Lio, and E. Bertolazzi. Combining safety margins and user preferences into a driving criterion for optimal control-based computation of reference maneuvers for an adas of the next generation. In IEEE Proceedings. Intelligent Vehicles Symposium, 2005., pages 36–41, 2005. doi: 10.1109/IVS.2005.1505074.

L. Brown, A. Morris, P. Thomas, K. Ekambaram, D. Margaritis, R. Davidse, D. S. Usami, M. Robibaro, L. Persia, I. Buttler, A. Ziakopoulos, A. Theofilatos, G. Yannis, A. Martin, and F. Wadji. Investigation of accidents involving powered two wheelers and bicycles – a european in-depth study. Journal of Safety Research, 76:135 – 145, 2021. doi: 10.1016/j.jsr.2020.12.015.

M. Diop, A. Boubezoul, L. Oukhellou, and S. Espié. Powered two-wheeler riding profile clustering for an in-depth study of bend-taking practices. Sensors, 20 (22), 2020. ISSN 1424-8220. doi: 10.3390/s20226696.

M. Diop, A. Boubezoul, L. Oukhellou, S. Espié, and S. Bouaziz. Powered two-wheelers right-hand curve negotiation study using segmentation and data mining approaches. IEEE Transactions on Intelligent Transportation Systems, 24(3):3407–3421, 2023. doi: 10.1109/TITS.2022.3222421.

T. Hastie, R. Tibshirani, J. H. Friedman, and J. H. Friedman. The elements of statistical learning: data mining, inference, and prediction, volume 2. Springer, 2009.

Y. Hisaoka, M. Yamamoto, and A. Okada. Closed-loop analysis of vehicle behavior during braking in a turn. JSAE Review, 20(4):537–542, 1999. ISSN 0389-4304. doi: 10.1016/S0389-4304(99)00042-9.

P. Huertas-Leyva, M. Nugent, G. Savino, M. Pierini, N. Baldanzini, and S. Rosalie. Emergency braking performance of motorcycle riders: skill identification in a real-life perception-action task designed for training purposes. Transportation Research Part F: Traffic Psychology and Behaviour, 63:93–107, 2019. ISSN 13698478. doi: 10.1016/j.trf.2019.03.019.

P. Huertas-Leyva, N. Baldanzini, G. Savino, and M. Pierini. Human error in motorcycle crashes: A methodology based on in-depth data to identify the skills needed and support training interventions for safe riding. Traffic Injury Prevention, 22(4):294–300, 2021. ISSN 1538957X. doi: 10.1080/15389588.2021.1896714. URL `https://www.tandfonline.com/doi/abs/10.1080/15389588.2021.1896714`.

H. Hurt, J. Ouellet, and D. Thom. Motorcycle accident cause factors and identification of countermeasures, volume 1: Technical report. Traffic Safety Center, University of Southern California, Los Angeles CA, USA, DOT-HS-805-862, 1, 01 1981.

R. Q. Ivers, C. Sakashita, T. Senserrick, J. Elkington, S. Lo, S. Boufous, and L. de Rome. Does an on-road motorcycle coaching program reduce crashes in novice riders? a randomised control trial. Accident Analysis & Prevention, 86:40–46, 2016. ISSN 0001-4575. doi: 10.1016/j.aap.2015.10.015.

D. Limebeer and M. Massaro. Dynamics and Optimal Control of Road Vehicles. 10 2018. ISBN 9780198825722; 9780198825715. doi: 10.1093/oso/9780198825715.001.0001.

R. Lot and J. Sadauckas. Motorcycle Design. Lulu.com, first edition, 2021.

N. Magiera, H. Janssen, M. Heckmann, and H. Winner. Rider skill identification by probabilistic segmentation into motorcycle maneuver primitives. In 2016 IEEE 19th International Conference on Intelligent Transportation Systems (ITSC), pages 379–386, 2016. doi: 10.1109/ITSC.2016.7795583.

M. Nugent, G. Savino, C. Mulvihill, M. Lenné, and M. Fitzharris. Evaluating rider steering responses to an unexpected collision hazard using a motorcycle riding simulator. Transportation Research Part F: Traffic Psychology and Behaviour, 66:292–309, 2019. ISSN 1369-8478. doi: https://doi.org/10.1016/j.trf.2019.09.005.

P. Savolainen and F. Mannering. Effectiveness of motorcycle training and motorcyclists' risk-taking behavior. Transportation Research Record, 2031:52–58, 12 2007. doi: 10.3141/2031-07.

P. Senin. Dynamic time warping algorithm review. Information and Computer Science Department University of Hawaii at Manoa Honolulu, USA, 855(1-23):40, 2008.

P. Terranova, M. E. Dean, C. Lucci, S. Piantini, T. J. Allen, G. Savino, and H. C. Gabler. Applicability assessment of active safety systems for motorcycles using population-based crash data: Cross-country comparison among australia, italy, and usa. Sustainability, 14(13), 2022. ISSN 2071-1050. doi: 10.3390/su14137563.

E. Vlahogianni, G. Yannis, J. C. Golias, N. Eliou, and P. Lemonakis. Identifying riding profiles parameters from high resolution naturalistic riding data. In Proceedings of the 3rd International Conference on Road Safety and Simulation (RSS2011), September, pages 14–16, 2011.

D. Weir. Motorcycle Handling Dynamics and Rider Control and the Effect of Design Configuration on Response and Performance. University of California, Los Angeles., 1972.

D. H. Weir and J. W. Zellner. Lateral-directional motorcycle dynamics and rider control. Publication of: Society of Automotive Engineers, 1978.

S. Will, B. Metz, T. Hammer, M. Mörbe, M. Henzler, F. Harnischmacher, and G. Matschl. Methodological considerations regarding motorcycle naturalistic riding investigations based on the use of g-g diagrams for rider profile detection. Safety Science, 129:104840, 2020. ISSN 0925-7535. doi: 10.1016/j.ssci.2020.104840.

R. A. Wilson-Jones. Steering and stability of single-track vehicles. Proceedings of the Institution of Mechanical Engineers: Automobile Division, 5(1):191–213, 1951. doi: 10.1243/PIME_AUTO_1951_000_023_02.